The Effect of Element Types on Force Analogy Method Analysis

Iraj Toloue*, Mohd Shahir Liew & Indra Sati Hamonangan Harahap

Civil and Environmental Engineering department, Universiti Teknologi PETRONAS, Bandar Seri Iskandar, 32610, Tronoh, Perak, Malaysia
*E-mail: toloue.iraj@gmail.com

Abstract. In this study, the seismic performance of a 2D portal frame subjected to the recorded seismic ground motions of the Northridge 1994 earthquake was evaluated by the force analogy method (FAM) with different element types. To increase the accuracy of FAM, Timoshenko (TS) elements were employed instead of the classical Euler Bernoulli (EB) elements, to revert the shear deformations that are neglected in EB elements. To perform evaluation, the same material and section properties were considered and the same portal frame was analyzed with different element lengths, from 0.5 to 7.0 m in 0.5 m steps.

Keywords: *earthquake; Euler-Bernoulli; FAM; nonlinear; Timoshenko.*

1 Introduction

The optimum design of frames, including their structure, requires precise system modeling and simulation to obtain an accurate structural response. Previous studies have indicated that beams and columns of any frame during extreme loading such as an earthquake usually face inelastic deformation. The most common practice in this area is to determine the changes of structural properties such as member stiffness. Although this method is precise, most users complain that it requires powerful computers and too much computational time.

The force analogy method (FAM) is a nonlinear analytical method that was first introduced in 1968 by Lin for analysis of the inelastic continuum mechanism and then developed by Wong and Li for analysis of nonlinear structures. FAM focuses on changes of displacement instead of stiffness [1-3]. This method considers a degree of freedom for each plastic hinge through the constant stiffness matrix. FAM can be utilized for a wide range of structures. Unlike traditional methods, FAM keeps the global stiffness matrix intact. The nonlinear behavior is determined through the relationship of the nonlinear displacement versus force. While in conventional methods the local stiffness matrix requires an update after each inelastic iteration, FAM implements an invariable stiffness matrix. In this way, the solution of the equation of motion can be formulated in

Received May 21st, 2017, Revised November 11th, 2017, Accepted for publication December 21st, 2017.
 ISSN: 2337-5779, DOI: 10.5614/j.eng.technol.sci.2017.49.6.6

explicit format by the state space method. The constant 2 x 2 n matrix in FAM saves a huge amount of storage memory and computational time [4,5]. FAM needs to inverse the mass matrix and hence the rotational mass moment of inertia in lumped mass systems is zero. Inversion of the mass matrix requires pre-condensation (shortening of the mass matrix). Moreover the condensed stiffness matrices remove the unnecessary DOF, which are located at the plastic hinges. These two modifications significantly reduce the computational cost [6,7].

The stability, accuracy and efficiency of FAM in representing inelastic behavior was evaluated on a real six-story hospital building in [8]. The efficiency of FAM in analyzing the impact of the 1994 Northridge earthquake on a six-story building was evaluated in [9]. The derived analytical plastic energy equations revealed an accurate energy response for the studied structure.

This nonlinear structural evaluation was continued by considering the P-delta effect, which is categorized as a geometric nonlinearity. This approach separates the inelastic deflection of a system from the total displacement and considers the recovery force and moment matrices to generate the FAM model. The process in comparison with conventional methods is more time-efficient and straightforward [10,11]. To strengthen a structure by reducing the lateral load, a concentrically braced frame (CBF) system was implemented in [12]. Physical theory in contrast with a finite element or phenomenological approach was chosen due to its balanced efficiency and accuracy. FAM coupled with state space formulations returned acceptable results for the numerical analysis when compared with prior experimental results on a braced frame element with 3 m height and 3 m width.

The efficiency of FAM has not only been proved for steel structures, but can also be applied on concrete structures. FAM was employed to analyze a concrete bridge structure subjected to time history earthquake loading in [13]. The results were verified against a numerical and an experimental test. As expected, the results were acceptable and time-efficient. FAM along with the state space formulation was implemented to evaluate the structural member failure on a RC framed structure in [14] and [15]. Based on the literature, in the construction of an inelastic element with a high level of accuracy it can be assumed that the plastic deformations are formed at zero length of the plastic zone at the two ends of the beam and column elements.

Li, *et al.* demonstrated that the equation of motion for a nonlinear MDOF system can be decoupled, while in the governing internal matrices, such as restoring force and moments in FAM, for structural members are not decomposable [16]. As a result of this finding, FAM can be used to determine

the basic parameters of each mode and solution of nonlinear 2D MDOF systems [17]. Further research proved that FAM is capable of analyzing a variety of structural types subjected to earthquake loading.

FAM is based on the classical Euler-Bernoulli (EB) beam theory. In this theory it is assumed that the plane section after deformation remains plane. In other words, the shear deformations in EB elements are neglected and assumed to be zero. EB elements were employed in all previous researches [2,5,8,10,18,19]. In its derivation it is assumed that the deflection of the beam is only due to the flexure and both shear and rotary inertia are neglected. Although Clough claimed that the proposed EB element is sufficient for the usual engineering models, the neglected shear effect in EB for deep beams leads to significant changes in the response and returns wrong values [20]. To solve this issue, the use of Timoshenko's (TS) beam theory releases one of EB's assumptions and lets the beam cross-section rotate along the beam axis. In other words, EB elements are a special case of TS elements [21].

In addition to the displacement differences between EB and TS elements, Wang studied the frequency differences between these two elements on a portal frame [22]. His analysis claimed significant differences on this issue. Jafari, *et al.* replaced the force-based EB element by the TS element in a geometrically nonlinear analysis to consider shear deformation and increase accuracy [23]. They tested the accuracy of the consistent flexibility matrix for large displacements through their extension method and found that the results were considerably accurate. The accuracy of analysis for frames analyzed by Timoshenko elements has been proved in several researches [24-27].

Although the frequency changes of these frames have been studied, there is no footprint of studying the displacement phase change during time history response. The present study aimed to make a benchmark for future researches for the benefits of using TS elements over EB elements. The main objective of this study was to show the effect of type of element on the analysis of a system based on FAM.

2 Methodology

Figure 1 illustrates the concept of FAM based on inelastic displacement. Basically, FAM extends initial stiffness 'k_l', from OA to applied static force 'F_a' at node 'B'. This point helps to define the elastic displacement '$X'(t)$' from point 'O' to 'B'. Subtraction of total displacement '$X(t)$' from elastic displacement results in inelastic displacement '$X''(t)$'. The mathematical form of the described concept is shown in Eq. (1):

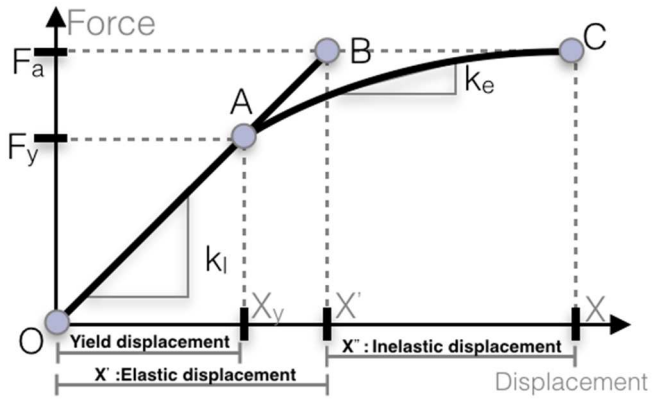

Figure 1 Force-displacement relationship.

$$X(t) = X'(t) + X''(t) \tag{1}$$

Consequently, the total system force 'F_a' is calculated based on Eq. (2):

$$\begin{aligned} F_a &= k_1 X' \\ &= k_1 (X - X'') \end{aligned} \tag{2}$$

The same concept generates total moment 'M' by elastic moment 'M'' and residual moment 'M'''. The mathematical form of the total moment is shown in Eq. (3):

$$M(t) = M'(t) + M''(t) \tag{3}$$

When an element enters into the inelastic region, plastic hinges, as described in Section 2, form at the two ends of the element. FAM assumes two imaginary matrices to restore the plastic rotations to zero. Applying these restoring matrices allow FAM to employ Hook's law in nonlinear analysis. The graph in Figure 2 displays the procedure of applying the restoring forces.

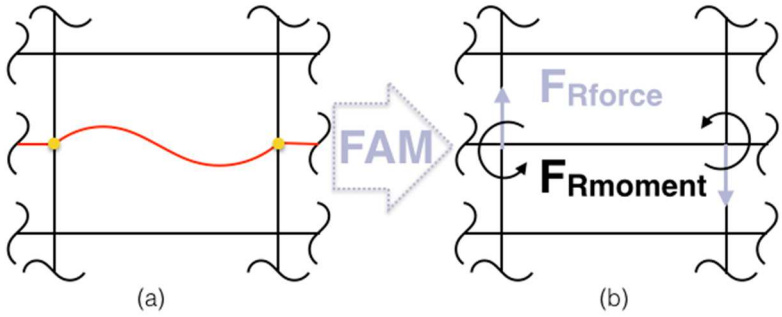

Figure 2 Restoring forces and moments.

FAM generates the restoring forces and moments based on stiffness matrix 'K' and relates them to plastic rotation vector 'θ'''. These relations are shown in Eqs. (4) and (5):

$$F_{Rforce} = -K_F\theta'' \tag{4}$$

$$F_{Rmoment} = -K_M\theta'' \tag{5}$$

K_F and K_M are member restoring force and moment based on the stiffness matrix. Solving the inelastic displacement based on the applied fictitious forces results in Eq. (6):

$$X''(t) = K^{-1}K_F\theta'' \tag{6}$$

The moment at the possible location of the plastic hinges is related to the restoring forces as shown in Eq. (7):

$$F_{Rmoment} = K_F^T K^{-1}K_F\theta'' \tag{7}$$

Finally, the residual moment 'M''', which is a combination of the restoring moment and the moment at the plastic hinge locations (PHLs) is shown in Eq. (8):

$$M'' = -(K_M - K_F^T K^{-1}K_F)\theta'' \tag{8}$$

FAM needs the equation of motion in state space form, as written in Eq. (9):

$$Z_{k+1} = F_d Z_k + H_d a_k + G_d X_k'' \tag{9}$$

where 'a_k' is the ground acceleration, 'H_d' is the effective earthquake node, and $Z = \begin{Bmatrix} x \\ \dot{x} \end{Bmatrix}$, $F_d = e^{A\Delta t}$, $A = \begin{bmatrix} 0 & I \\ -K/M & -C/M \end{bmatrix}$, $G_d = \begin{bmatrix} 0 \\ K/M \end{bmatrix}$. 'M', 'K', and 'C' are the mass, stiffness and damping matrices of the system. In our study, the stiffness matrix for FAM is generated based on the Euler-Bernoulli element. The stiffness matrices for EB and TS elements are shown in Eqs. (10) and (11):

$$K_{EB} = \begin{bmatrix} \frac{12EI}{L^3} & & & \\ \frac{6EI}{L^2} & \frac{4EI}{L} & & \\ -\frac{12EI}{L^3} & -\frac{6EI}{L^2} & \frac{12EI}{L^3} & \\ \frac{6EI}{L^2} & \frac{2EI}{L} & -\frac{6EI}{L^2} & \frac{4EI}{L} \end{bmatrix} \tag{10}$$

$$K_{TS} = \begin{bmatrix} k_1 & & & \\ k_2 & k_3 & & \\ -k_1 & -k_2 & k_1 & \\ k_2 & k_4 & -k_2 & k_3 \end{bmatrix} \tag{11}$$

where,

$$k_1 = \frac{12EI}{L^3(1+\varphi)}, k_2 = \frac{6EI}{L^2(1+\varphi)}, k_3 = \frac{(4+\varphi)EI}{L(1+\varphi)}, k_3 = \frac{(2-\varphi)EI}{L(1+\varphi)}, \varphi = \frac{12EI}{G\frac{A}{\kappa}L^2}$$

In Eqs. (10) and (11), modulus of elasticity, section area, length of the beam, shear modulus, inertia moment, and TS coefficient are represented by E, A, L, G, I, and κ, respectively.

3 Case Study

The proposed algorithm was applied on a two-dimensional portal frame with the same height and width 'L' as shown in Figure 3(a). To study the nonlinear behavior according to FAM, six possible PHLs based on the literature were considered on both ends of the frame's elements. As changes of length have a huge impact on the element type, 14 different cases of 'L', from 0.5 to 7 m were evaluated in this study. The algorithm writing was executed in MATLAB on Windows 8, i5 CPU, with 4 Gb of RAM. It was once executed using EB elements and once using TS elements. The average computational time for nonlinear analysis based on FAM was recorded as 1.319 sec. Only one hollow square cross section (see Figure 3(b)) was used in all of the cases for both beams and columns. The details of the section properties are shown in Table 1.

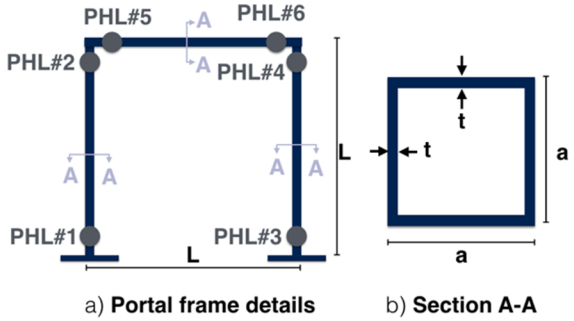

Figure 3 Frame details.

Table 1 Section properties.

Description	Symbol	Value	Unit
Modulus of elasticity	E	200	GPa
Thickness	T	0.001	m
Width (height)	a	0.209	m
Area	A	8.3202	cm^2
Moment of inertia	I	6×10^{-6}	m^4
Timoshenko coefficient	κ	5/6	--

Finally, to push the system in a nonlinear region, the recorded seismic ground motions from the 1994 Northridge earthquake, shown in Figure 4, were applied to the frame.

4 Results and Discussion

To illustrate the effect of element type on the analysis results, the two-dimensional frame from [3] was selected as a reference point. The frame had elements with a length of 4 m and was analyzed with FAM. The ground acceleration of the modified 1994 Northridge earthquake was imposed (the modification of the data is not provided in the reference) and it was tried to get the best fit between the digitized data and plot and the original earthquake from the Pacific Earthquake Engineering Research (PEER) center as shown in Figure 4. Finally, in this study, PEER data were used as trusted earthquake acceleration data.

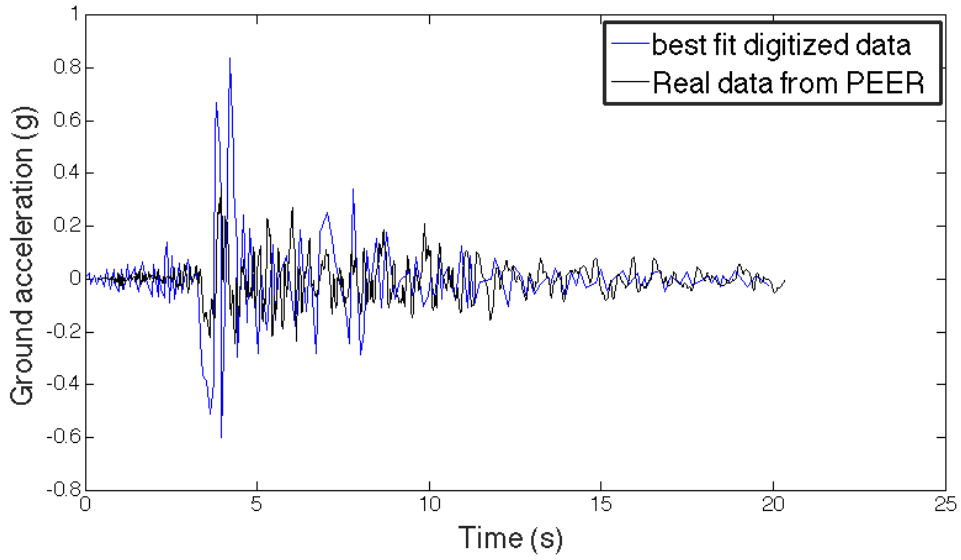

Figure 4 1994 Northridge earthquake.

The example in Li and Wong [3] was modeled using the same steps and the results of the algorithm were almost same as those in the reference. The slight differences between the results were due to the mismatch between the real and the digitized ground motion. The same steps were executed using TS elements; the results are plotted in Figure 5. On the whole, at this length, the results of TS and EB elements for linear and nonlinear displacement and the plastic hinge rotations overlapped almost exactly. The results in this section always refer to the example from [3] as the benchmark.

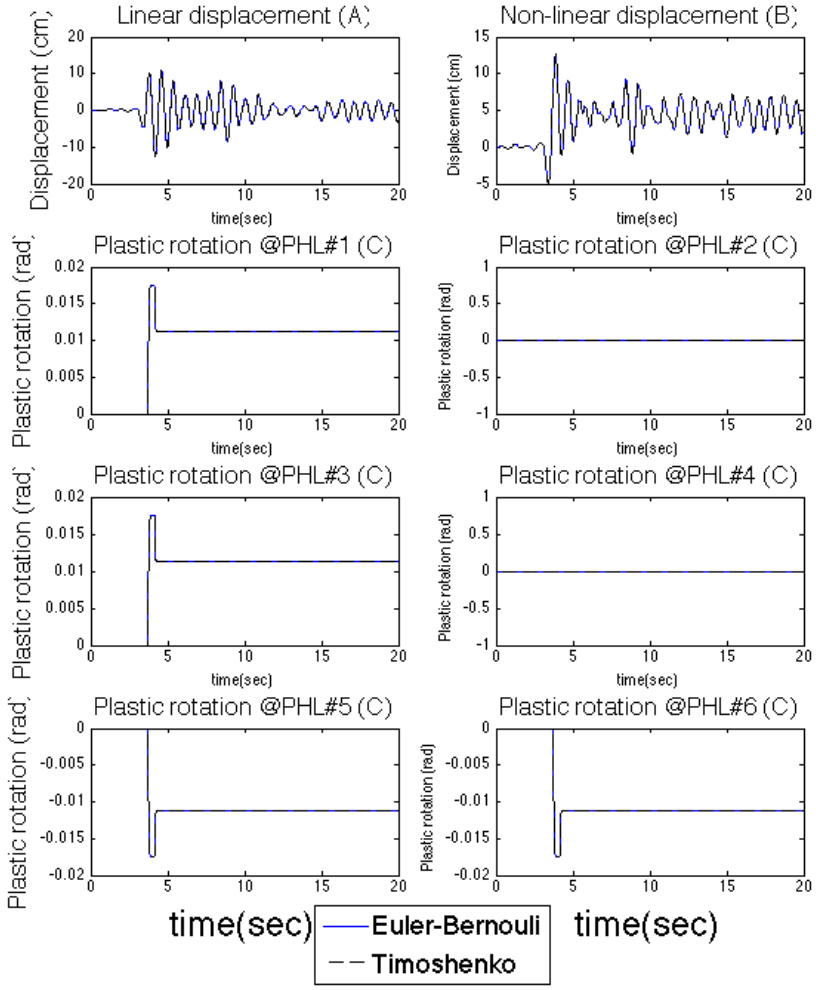

Figure 5 Frame with 4-m elements.

As the aim of this study was to compare the response of the system analyzed using EB and TS elements, the same steps were executed with different frame lengths from 0.5 to 7 m. The maximum linear and nonlinear differences between the EB and TS elements with respect to their length (difference/length) are displayed in Figure 6.

In contrast with conventional belief, which holds that the differences between the assumptions of EB and TS elements are reduced when the length increases, Figure 6 reveals that these differences fluctuate along the increase of the

members' length. For the first five frames (0.5 to 2.5 m), as expected, the Timoshenko results were consistently higher than EB's. At 3-m frame length, the sign changed and EB was larger than TS. The oscillation of the results in sign and ratio breaks the classical belief on frame analysis using TS elements.

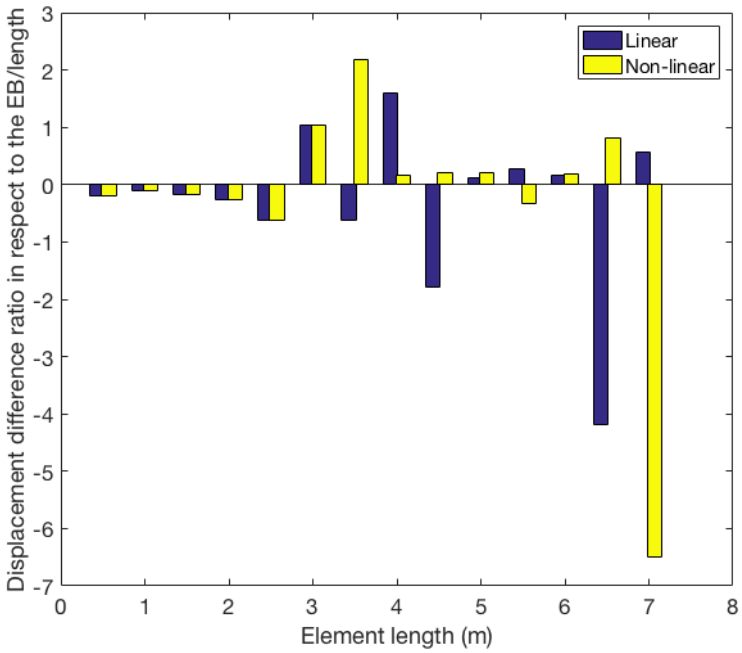

Figure 6 Displacement difference ratio with respect to the EB/length.

In the same way, the six plastic hinge locations for all of the 14 cases are presented in Figure 7. Again, the value of PHL ratio with respect to frame length fluctuated when the element length was increased. For frames with an element length of 2 m and 6 m the differences were negligible. However, in most cases EB showed higher rotation, while in some of the cases, such as element length at 4.5 m and 6 m, TS was higher.

The difference between TS and EB in reference with EB are shown in Figure 8. Not only do the results show fluctuation, a boom occurs at the 7-m frame. The results of the 7-m frame are shown in Figure 9. The discrepancies between TS and EB can be clearly seen during the occurrence of the earthquake.

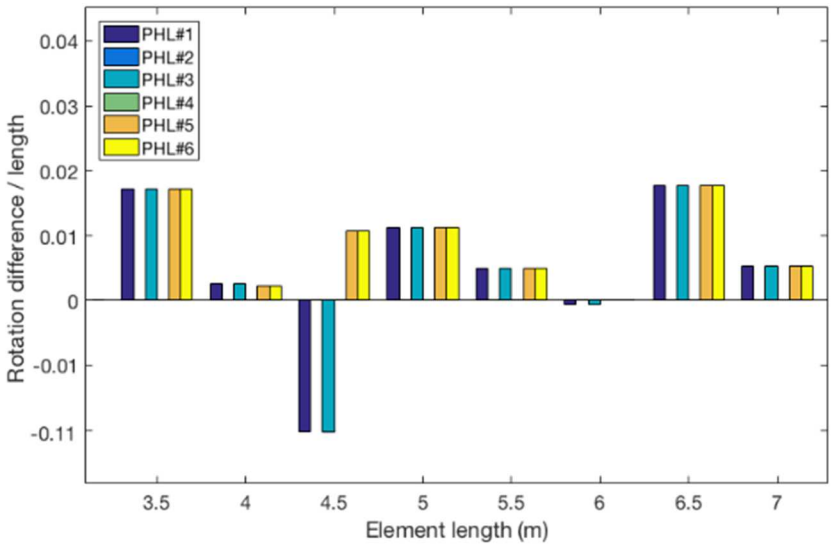

Figure 7 Rotation difference ratio with respect to the EB/length.

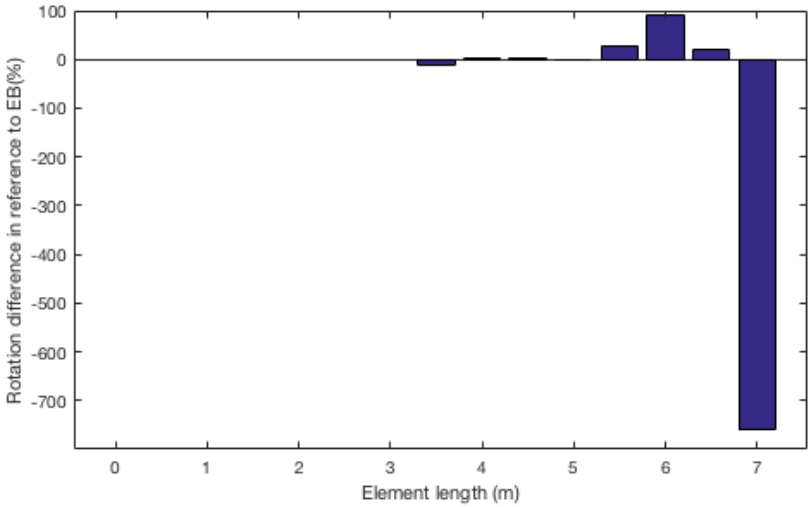

Figure 8 Rotation difference in reference with EB.

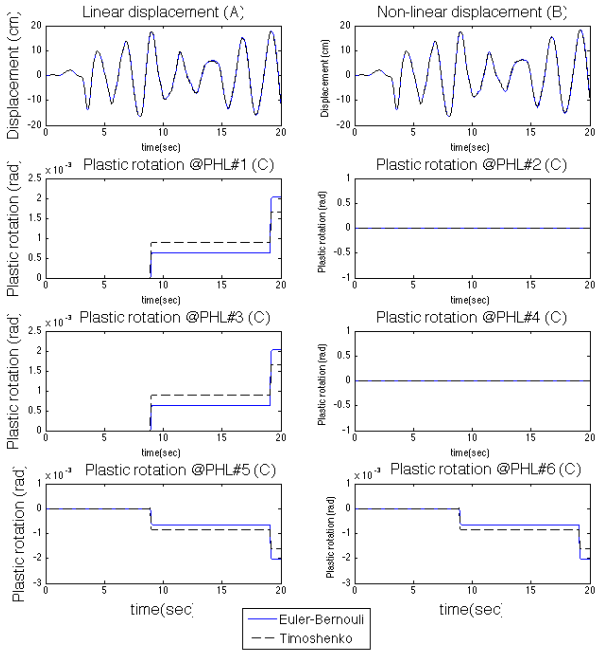

Figure 9 Frame with 7-m element.

The dynamic characteristics of the frame with EB and TS elements are shown in Table 2. The table reveals that the natural frequency of the frame generated by TS was slightly smaller than for EB. Furthermore, this difference gradually decreased while the frame's length was increased.

Table 2 Dynamic characteristics.

L(m)	ω_{EB}	ω_{TS}	$\Delta\omega\%$
0.5	507	436	14
1.0	127	121	4.1
2.0	31.74	31.40	1.1
2.5	20.31	20.17	0.71
3.0	14.11	14.04	0.49
3.5	10.36	10.32	0.36
4.0	7.93	7.91	0.27
4.5	6.27	6.25	0.22
5.0	5.08	5.07	0.17
5.5	4.19	4.192	0.14
6.0	3.52	3.523	0.12
6.5	3.005	3.002	0.1
7.0	3.59	3.59	0

The hysteresis loops of three different frame lengths of 4, 5.5 and 6.5 m for PHL#1 are illustrated in Figure 10. While the frame length increased, a more obvious violation was detected in the hysteresis loops.

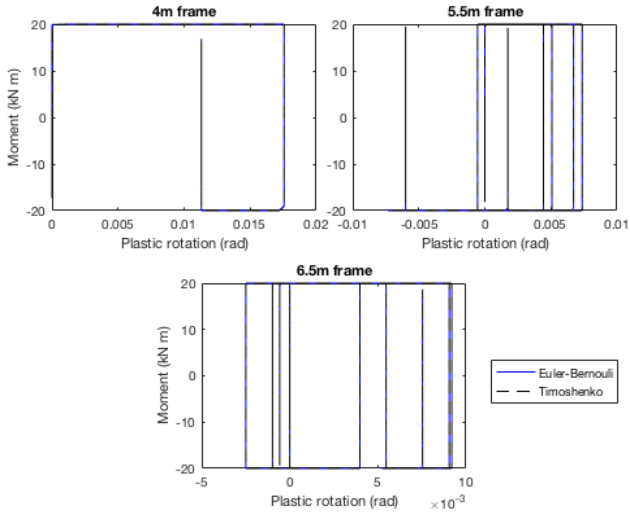

Figure 10 Hysteresis loops for PHL#1.

The paths of these hysteresis loops suggest further study on the control system where the phase of the system may change.

5 Conclusion

In this study, an attempt was made to show the effect of element type on the response of FAM. Several frames with different element lengths were analyzed. The detected differences when L was increased were irregular and did not follow any pattern. The differences between TS and EB elements in some of the cases, such as at 4-m element length, were negligible while in others it was not. Although the displacement changes are not significant for engineering purposes, the magnitudes of the displacement changes in the time history record suggest further study on the replacement of EB elements by TS elements in nonlinear control systems.

Reference

[1] Lin, T.H., *Theory of Inelastic Structures*, John Wiley & Sons, New York, NY, USA, 1968.

[2] Hart, G.C. & Wong, K., *Structural Dynamics for Structural Engineers*, John Wiley and Sons, 2000.
[3] Li, G. & Wong, K.K., *Theory of Nonlinear Structural Analysis*, John Wiley & Sons, Singapore Pte. Ltd., Chi Chester, UK, 2014.
[4] Qu, J-T. & Li, H-N., *Study on Optimal Placement and Reasonable Number of Viscoelastic Dampers by Improved Weight Coefficient Method,* Mathematical Problems in Engineering, **2013**, Article ID 358709, 10 p., 2013.
[5] Zhang, Y., *Seismic Performance Assessment of Offshore Reinforced Concrete Bridges Using the Force Analogy Method*, International Journal of Structural Stability and Dynamics, **16**(5), 1550012, pp.31-46, 2016.
[6] Wong, K.K.F. & Wang, Y., *Energy-based Design of Structures Using modified force analogy method*, The Structural Design of Tall and Special Buildings, **12**(5), pp. 393-407, 2003.
[7] Wong, K.K.F. & Wang, Z., *Seismic Analysis of Inelastic Moment-resisting Frames Part I: Modified Force Analogy Method for End Offsets*, The Structural Design of Tall and Special Buildings, **16**(3), pp. 267-282, 2007.
[8] Wong, K.K.F. & Yang, R., *Inelastic Dynamic Response of Structures using Force Analogy Method*, Journal of Engineering Mechanics, **125**(10), pp. 1190-1199, 1999.
[9] Wong, K.K.F. & Yang, R., *Earthquake Response and Energy Evaluation of Inelastic Structures*, Journal of Engineering Mechanics, **128**, pp. 308-317, 2002.
[10] Zhao, D. & Wong, K.K., *New Approach for Seismic Nonlinear Analysis of Inelastic Framed Structures*, Journal of Engineering Mechanics, **132**(9), pp. 959-966, 2006.
[11] Chao, S.H. & Loh, C.H., *Inelastic Response Analysis of Reinforced Concrete Structures using Modified Force Analogy Method*, Earthquake Engineering & Structural Dynamics Structural Dynamics, **36**(12), pp. 1659-1683, 2007.
[12] Li, G., Fahnestock, A.L. & Li, H.-N., *Simulation of Steel Brace Hysteretic Response using the Force Analogy Method*, Journal of Structural Engineering, **139**(4), pp. 526-536, 2013.
[13] Li, G., Zhang, Y. & Li, H.-N., *Nonlinear Seismic Analysis of Reinforced Concrete Bridges Using the Force Analogy Method*, Journal of Bridge Engineering, **20**(10), pp. 04014111, 2014.
[14] Li, G., Zhang, Y. & Li, H.-N., *Seismic Damage Analysis of Reinforced Concrete Frame Using the Force Analogy Method*, Journal of Engineering Mechanics, **139**(12), pp. 1780-1789, 2013.

[15] Li, G., Zhang, Y. & Li, H.-N., *Nonlinear Seismic Analysis of Reinforced Concrete Frames using the Force Analogy Method, Earthquake Engineering & Structural Dynamics*, **43**(14), pp. 2115-2134, 2014.

[16] Li, G., Li, H-N. & Zhang, Y., *Displacement Estimation of Nonlinear Structures Using the Force Analogy Method*, Structural Design of Tall and Special Buildings, **24**, pp. 59-72, 2015.

[17] Chuan-guo, Y., Chun-guang, L. & Chun-xu, X., *Application of Force analogy Method in Seismic Response of Structures*, Journal of Water Resources and Architectural Engineering, **3**(3), pp. 72-75, 2014.

[18] Villaverde, R., *Simplified Response – Spectrum Seismic Analysis of Nonlinear Structures*, Journal of Engineering Mechanics, **122**(3), pp. 282-285, 1996.

[19] Li, G. & Li, H-N., *Seismic Response Analysis of Structure with Energy Dissipation Devices Using Force Analogy Method*, The Structural Design of Tall and Special Buildings, **20**, pp. 291-313, 2011.

[20] Clough, R.W., *On the Importance of Higher Modes of Vibration in the Earthquake Response of a Tall Building*, Bulletin of the Seismological Society of America, **45**(4), pp. 289-301, 1955.

[21] Luo, Y., *An Efficient 3D Timoshenko Beam Element Homogeneous Euler-Lagrangian Equations Governing 3D Timoshenko Beam*, **1**(3), pp. 95-106, 2008.

[22] Wang, T.M. & Kinsman, T.A., *Vibrations of frame structures According to the Timoshenko Theory*, Journal of Sound and Vibration, **14**(2), 215-227, 1971.

[23] Jafari, V., Vahdani, S. & Rahimian, M., *Derivation of the Consistent Flexibility Matrix for Geometrically Nonlinear Timoshenko Frame Finite Element*, Finite Elements in Analysis and Design, **46**(12), pp. 1077-1085, 2010.

[24] Kounadis, A.N., *Dynamic Snap-through Buckling of a Timoshenko Two Bar Frame under a Suddenly Applied Load*, Zeitschrift fur Angewandte Mathematik und Mechanik (ZAMM), **59**(10), pp. 523-531, 1979.

[25] Pavan Kumara, B. & Murigendrappa, S.M., *Theoretical and Numerical Studies on In-Plane Free Vibration of Two-Member Timoshenko Frame with Open Crack*, National Conference on Advances in Mechanical Engineering Science (NCAMES), pp. 237-243, 2016.

[26] Dragovic´, V. & Gajic´, B., *Some Recent Generalizations of the Classical Rigid Body Systems*, Arnold Mathematical Journal, **2**(4), pp. 511-578, 2016.

[27] Wang, R. & Jeng, J., *Dynamic Analysis of a t Type Timoshenko Frame to a Moving Load using Finite Element Method*, Journal of the Chinese Institute of Engineers, **19**(3), pp. 409-416, 1996.